




Upper bound for entropy production in Markov processes

Tomohiro Nishiyama *
Tokyo 206-0003, Japan

Yoshihiko Hasegawa †
Department of Information and Communication Engineering, Graduate School of Information Science and Technology,
University of Tokyo, Tokyo 113-8656, Japan

 (Received 7 August 2023; accepted 4 October 2023; published 24 October 2023)

The second law of thermodynamics states that entropy production cannot be negative. Recent developments concerning uncertainty relations in stochastic thermodynamics, such as thermodynamic uncertainty relations and speed limits, have yielded refined second laws that provide lower bounds of entropy production by incorporating information from current statistics or distributions. In contrast, in this study we bound the entropy production from above by terms comprising the dynamical activity and maximum transition-rate ratio. We derive two upper bounds: One applies to steady-state conditions, whereas the other applies to arbitrary time-dependent conditions. We verify these bounds through numerical simulation and identify several potential applications.

DOI: [10.1103/PhysRevE.108.044139](https://doi.org/10.1103/PhysRevE.108.044139)

I. INTRODUCTION

The second law of thermodynamics is considered one of the most fundamental and universal principles in physics and the cornerstone of many scientific disciplines. It states that in any physical process, the entropy production of the system either increases or remains unchanged but never decreases. The second law of thermodynamics was recently refined in stochastic thermodynamics through uncertainty relations, which have garnered attention in stochastic thermodynamics. One commonly cited example is the thermodynamic uncertainty relation (TUR) [1–20]. The TUR states that achieving greater accuracy in thermodynamic systems comes at the cost of increased thermodynamic expenditures, such as entropy production or dynamical activity. Furthermore, the TUR gives a bound for current fluctuations by the entropy production (or the dynamical activity). From a different perspective, the TUR provides lower bounds of the entropy production, which are refinements of the second law of thermodynamics. Specifically, the TUR states that

$$\Sigma \geq \frac{2\mathbb{E}[J]^2}{\text{Var}[J]} \geq 0, \quad (1)$$

where Σ is the entropy production, J is the thermodynamic current (see Sec. III for a detailed definition), and $\mathbb{E}[\cdot]$ and $\text{Var}[J]$ denote the expectation value and variance, respectively. Equation (1) provides a tighter bound to the conventional second law by using additional information regarding the current. Another related uncertainty relation in stochastic thermodynamics is the classical speed limit (CSL) [21–27]. The CSL is a classical generalization of the quantum speed limit [28–30],

which places a limit on the speed of state change. An instance of the CSL is given by

$$\Sigma \geq k\mathcal{W}(P(\tau), P(0)), \quad (2)$$

where $P(0)$ and $P(\tau)$ are the initial and final densities, respectively, $\mathcal{W}(\cdot, \cdot)$ is the Wasserstein distance between the probability densities at $t = 0$ and $t = \tau$, and k is a constant that does not depend on state. As with Eq. (1), the CLS gives a lower bound of the entropy production and thus can be identified as an improved second law.

As demonstrated above, while the lower bound of entropy production has received considerable attention in uncertainty relations, its upper bound has been less explored. The lower bound of the entropy production is of practical significance in thermodynamic inference because this method estimates entropy production based on trajectory measurements [31–33]. However, the precision of these estimations remains relatively low for realistic cases. Reference [34], for example, estimated the entropy production based on a biological model; however, the numbers are often off by two or three digits. Therefore, if the upper bound is available, its inclusion can lead to more accurate estimates of the entropy production. Moreover, once the upper bound of the entropy production can be derived, several inequalities, such as Eqs. (1) and (2), have an alternative upper bound other than the entropy production. The upper bound for the average entropy production was studied in Ref. [35], which is based on extrema of the entropy production [36]. Reference [37] derived an upper bound of quantum entropy production with the entropy flux rate. Reference [38] derived a reversed TUR which gives an upper bound to the entropy production by the work exerted on a bead.

In the present study, using results from Ref. [39], we show that entropy production can be bounded from above by the terms comprising the dynamical activity [cf. Eq. (5)] and the maximum ratio between any pair of transition rates

*htam0ybboh@gmail.com

†hasegawa@biom.t.u-tokyo.ac.jp

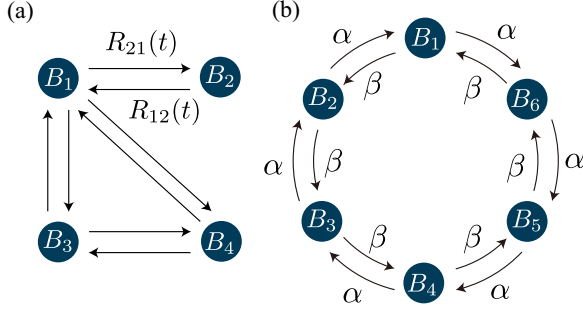


FIG. 1. (a) Example of Markov processes considered in this study. The $R_{nm}(t)$ denote the transition rates from B_m to B_n at time t . If the transition from B_m to B_n is possible, then the transition in the opposite direction should also be possible, which is a requirement for defining entropy production. (b) Markov process with a ring topology that achieves the equality condition of Eq. (8). Here $\alpha > 0$ and $\beta > 0$ represent the transition rates for the clockwise and counterclockwise directions, respectively.

[cf. Eq. (6)]. We derive two upper bounds, one that applies to steady-state conditions and another that applies to arbitrary time-dependent driven conditions. The latter bound appears to hold for general Markov processes with time-dependent transition rates, starting from any probability distribution. By considering a long-time limit with time-independent transition rates, it can be shown that the latter bound reduces to the former steady-state bound. We verify the obtained bounds using a numerical simulation. Moreover, we present possible applications of the obtained bounds.

II. METHOD AND RESULTS

Consider a classical Markov process comprising N states $\{B_1, B_2, \dots, B_N\}$. Let $R_{nm}(t)$ be the transition rate from B_m to B_n at time t and let $P_m(t)$ be the probability of being B_m at time t . The dynamics is supposed to obey the master equation

$$\frac{d}{dt}P_n(t) = \sum_m R_{nm}(t)P_m(t), \quad (3)$$

where we define the diagonal elements as $R_{mm}(t) \equiv -\sum_{n \neq m} R_{mn}(t)$. We assume that if $R_{nm}(t) > 0$ for any indices m and n satisfying $m \neq n$, then $R_{mn}(t) > 0$ [Fig. 1(a)]. Then, assuming local detailed balance, we can define the entropy production rate $\sigma(t)$ and dynamical activity rate $\alpha(t)$ at time t :

$$\sigma(t) \equiv \sum_{n < m} [P_m(t)R_{nm}(t) - P_n(t)R_{mn}(t)] \ln \frac{P_m(t)R_{nm}(t)}{P_n(t)R_{mn}(t)}, \quad (4)$$

$$\alpha(t) \equiv \sum_{n < m} [P_m(t)R_{nm}(t) + P_n(t)R_{mn}(t)]. \quad (5)$$

Here the dynamical activity rate $\alpha(t)$ quantifies the average number of jumps at time t . Moreover, we define the ratio R , which quantifies the maximum ratio between any pair of transition rates $R_{nm}(t)$:

$$R \equiv \max_{n \neq m, t} \frac{R_{nm}(t)}{R_{mn}(t)} \geq 1. \quad (6)$$

Note that, when $R_{nm} = R_{mn} = 0$, we define $R = 1$. When the system is time independent, Eq. (6) reduces to

$$R = \max_{n \neq m} \frac{R_{nm}}{R_{mn}} \geq 1. \quad (7)$$

A. Steady-state case

We first consider a time-independent Markov process (i.e., R_{nm} is time independent) and assume that the system is in the steady state with P_m^{ss} the steady-state distribution, where $\sigma(t) = \sigma$ and $\alpha(t) = \alpha$. Under steady-state conditions, we obtain the following upper bound on the entropy production rate:

$$\sigma \leq \alpha(\ln R) \frac{R-1}{R+1}. \quad (8)$$

Equation (8) is the first main result of this study and its proof is provided in Appendix A. Equation (8) provides an upper bound on the entropy production σ in terms of the dynamical activity α and the ratio R [Eq. (7)]. Let us consider the equality case of Eq. (8). Equation (8) becomes an equality when the entropy production and dynamical activity rates are given by

$$\alpha = c(\alpha + \beta), \quad \sigma = c(\beta - \alpha) \ln \frac{\beta}{\alpha} \quad (9)$$

for the transition rates $\alpha > 0$ and $\beta > 0$ and constant $c > 0$. Consider a Markov process with a ring topology, where the transition rates in the clockwise and counterclockwise directions are denoted by α and β , respectively [Fig. 1(b)]. Such a Markov process has been extensively studied in stochastic clock models [40]. The entropy production and dynamical activity of the ring system are given by Eq. (9) and hence Eq. (8) is saturated in the system.

Equation (8) is meaningful from a practical point of view. Equation (8) shows that the ratio σ/α can be bounded from above by R alone. Since the measurement of R is relatively easy, Eq. (8) can be used to infer the ratio σ/α from measurements of stochastic trajectories.

B. Time-dependent driven case

We have so far obtained the upper bound for entropy production for the steady-state case. Next we derive the upper bound for entropy production in a time-dependent driven process. Suppose that the process begins at $t = 0$ and ends at $t = \tau$ ($\tau > 0$). Let $\Sigma(\tau)$ and $\mathcal{A}(\tau)$ be the entropy production and dynamical activity, respectively, within the interval $[0, \tau]$:

$$\Sigma(\tau) \equiv \int_0^\tau dt \sigma(t), \quad (10)$$

$$\mathcal{A}(\tau) \equiv \int_0^\tau dt \alpha(t). \quad (11)$$

Here $\Sigma(\tau)$ quantifies the entropy production generated during the interval $[0, \tau]$ and $\mathcal{A}(\tau)$ denotes the average number of jump events during $[0, \tau]$. Then we obtain upper bounds on the entropy production as follows:

$$\Sigma(\tau) \leq \mathcal{A}(\tau) (\ln R) \frac{R-1}{R+1} + \left(1 + \frac{2R \ln R}{R^2 - 1}\right) \ln N. \quad (12)$$

Equation (12) is the second result of this study, which holds for an arbitrary Markov process starting from an arbitrary

state. Equation (12) shows that the upper bound of the entropy production is determined solely by $\mathcal{A}(\tau)$, R , and N . Note that (12) trivially holds for $\Sigma(\tau) \leq [1 + (\ln R)/(R + 1)] \ln N$. A proof for Eq. (12) is provided in Appendix B. The bound of Eq. (12) tightens when $\Sigma(\tau) \gg \ln N$. Under this condition, Eq. (12) converges to the same inequality as derived for the steady-state case [Eq. (8)]. Therefore, in addition to $\Sigma(\tau) \gg \ln N$, the conditions given by Eq. (9) are required for a saturation of the bound of Eq. (12).

C. Numerical simulation

Before providing applications, we verify the upper bounds [Eqs. (8) and (12)] via numerical simulation. In this respect, we randomly generate Markov processes (time-independent transition rates R_{nm}) and calculate the entropy production rate σ and its upper bounds. For details of the simulation parameters, see the caption of Fig. 2. Figure 2(a) illustrates Eq. (8), which is the upper bound for the steady-state condition by showing the entropy production rate $\sigma(\tau)$ as a function of the right-hand side of Eq. (8), where the points represent random realizations and the solid line represents the saturating case. When Eq. (8) is satisfied, all points should be located above the solid line. As can be seen, all the points are above the line, indicating that Eq. (8) holds for the simulation. We also check whether Eq. (8) holds for out-of-steady-state dynamics. In Fig. 2(b) we select random initial probability distributions and calculate the same quantities as in Fig. 2(a). We see that some points are below the solid line, implying that the steady-state bound [Eq. (8)] is not satisfied for the out-of-steady-state case.

Next we verify the bound for the out-of-steady-state condition [Eq. (12)]. Figure 2(c) visualizes Eq. (12), where $\Sigma(\tau)$ is plotted as a function of the right-hand side of Eq. (12). In Fig. 2(c) the points denote random realizations and the solid lines represent the saturating cases of Eq. (12). Clearly, all points are located above the solid lines, numerically verifying the obtained bounds. Since Eq. (12) is trivially valid when $\Sigma(\tau) \leq [1 + (\ln R)/(R + 1)] \ln N$, its tightness is weaker than the steady-state case [Eq. (8)], which can be confirmed by comparing Figs. 2(a) and 2(c).

III. EXAMPLES

In the first two examples, we show the new upper bounds for the precision of the generic current and the probability of entropy production.

A. Precision of generic current

We consider a system that is controlled by an arbitrary protocol $\lambda(vt)$ with speed parameter v and let $R_{nm}(t) = R_{nm}(\lambda(vt))$ for all m and n . Let $\omega_\tau = \{n_0, (n_1, t_1), \dots, (n_K, t_K)\}$ be a stochastic trajectory of the system during the time interval $[0, \tau]$, where the system is initially in state n_0 and a transition from state n_{i-1} to state n_i occurs at time t_i for each $1 \leq i \leq K$. For each trajectory, we consider the generic current $J = J_d(\omega_\tau) \equiv \sum_{i=1}^K d_{n_i n_{i-1}}$ for antisymmetric coefficient $d_{mn} = -d_{nm}$ and we define the precision of the generic current as $\mathfrak{p}(J) \equiv (\nabla \mathbb{E}[J])^2 / \text{Var}[J]$. Here $\nabla \equiv \tau \partial_\tau - v \partial_v$ is a differential operator, and $\mathbb{E}[\cdot]$ and $\text{Var}[\cdot]$ denote the ensemble average and variance

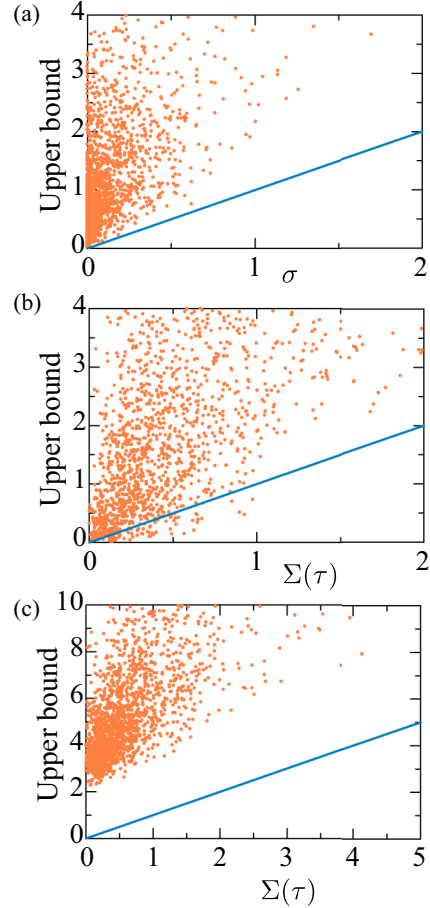


FIG. 2. Numerical simulation of the upper bounds of entropy production. (a) Right-hand side of Eq. (8) as a function of σ under the steady-state condition. Random realizations are plotted by points and the solid line denotes the equality case. (b) Right-hand side of Eq. (8) as a function of σ under non-steady-state conditions. Since Eq. (8) assumes the steady-state condition, the bound is not expected to hold under non-steady-state conditions. The points and the solid line have the same meanings as those of (a). (c) Right-hand side of Eq. (12) as a function $\Sigma(\tau)$ under non-steady-state conditions. The number of states is randomly sampled from $\{3, 4, 5\}$ and the transition rate R_{nm} is randomly determined. In (a) the initial probability is P_m^{ss} . In (b) and (c) the initial probability $P_m(0)$ is randomly sampled and the time duration τ is sampled from $[0.1, 5]$.

of the current, respectively. Using the thermodynamic and kinetic uncertainty relation in Ref. [39], we obtain

$$\frac{\mathfrak{p}(J)}{\mathcal{A}(\tau)} \leq \frac{\Sigma(\tau)^2}{4\mathcal{A}(\tau)^2 f\left(\frac{\Sigma(\tau)}{2\mathcal{A}(\tau)}\right)^2}, \quad (13)$$

where $f(x)$ is the inverse function of $x \tanh x$. Combining $g(x) = x/f(x)$, where $g: [0, \infty) \rightarrow [0, 1)$ is the inverse function of $x \tanh^{-1} x$ in Ref. [41], we obtain

$$\frac{\mathfrak{p}(J)}{\mathcal{A}(\tau)} \leq g\left(\frac{\Sigma(\tau)}{2\mathcal{A}(\tau)}\right)^2. \quad (14)$$

Since g increases monotonically, by combining Eqs. (8) and (12), it follows that

$$\frac{p(J)}{\mathcal{A}(\tau)} \leq g \left[\frac{\ln R}{2} \left(\frac{R-1}{R+1} \right) + \frac{C}{2\mathcal{A}(\tau)} \right]^2, \quad (15)$$

where the constant C on the right-hand side is equal to zero for the steady-state case and $C = (1 + 2R \ln R / (R^2 - 1)) \ln N$ for the time-dependent driven case. Since $|g(x)| < 1$ for all non-negative x , this inequality is tighter than the kinetic uncertainty relation $p(J)/\mathcal{A}(\tau) \leq 1$ in [5]. For the steady-state case, note that the right-hand side of Eq. (15) depends only on R , which is determined by the system. When $d_{mn} = 1$ for $n < m$, since $\mathbb{E}[J] = c\tau(\beta - \alpha)$ and $\text{Var}[J] = c\tau(\alpha + \beta)$ hold in the case presented in Fig. 1(b), Eq. (15) becomes the equality.

B. Probability of entropy production

We derive an upper bound for the probability that the entropy production is greater than or equal to a given value $s \geq 0$. We also derive an upper bound for the probability that the entropy production is less than or equal to s . We assume that the strong detailed fluctuation theorem holds, $P(\Sigma)/P(-\Sigma) = e^\Sigma$, where $P(\Sigma)$ is the probability of entropy production Σ . To satisfy this condition, the system must meet two requirements [42]. First, the initial and final probability distributions must agree. Second, the external protocol must be time symmetric. Since $\phi(\Sigma) \equiv \Sigma[1 - \exp(-\Sigma)]$ is nondecreasing and non-negative for $\Sigma \geq 0$, we obtain

$$\begin{aligned} \phi(s)P(\Sigma \geq s) &\leq \int_s^\infty d\Sigma \phi(\Sigma)P(\Sigma) \\ &\leq \int_0^\infty d\Sigma \phi(\Sigma)P(\Sigma) \\ &= \int_{-\infty}^\infty d\Sigma \Sigma P(\Sigma) = \Sigma(\tau), \end{aligned} \quad (16)$$

where we use $P(-\Sigma) = \exp(-\Sigma)P(\Sigma)$. By combining this relation with the upper bounds [Eqs. (8) and (12)], we obtain

$$P(\Sigma \geq s) \leq \frac{\mathcal{A}(\tau)(\ln R)\left(\frac{R-1}{R+1}\right) + C}{s[1 - \exp(-s)]}, \quad (17)$$

where the definition of C is the same as in the example in Sec. III A. From Eq. (17) we obtain

$$\begin{aligned} P(\Sigma \leq -s) &= \int_s^\infty d\Sigma \exp(-\Sigma)P(\Sigma) \\ &\leq \exp(-s)P(\Sigma \geq s) \\ &\leq \frac{\mathcal{A}(\tau)(\ln R)\left(\frac{R-1}{R+1}\right) + C}{s(\exp(s) - 1)}. \end{aligned} \quad (18)$$

C. Arrow of time inference

As an example of the entropy-production upper bound, we consider the inference of the arrow of time from trajectory measurements [43,44]. Suppose that two movies are shown. The first is a forward movie depicting a system that undergoes a process in which the external protocol λ changes from A to B . The other is a backward movie that displays the reverse process, where λ goes from B to A , and is being played backward.

The initial distribution of the backward process is identical to the final probability of the forward process, as assumed in the fluctuation theorem. Our task is to guess whether this movie is the forward or backward movie. It is known that the likelihood of the forward process given a trajectory ω_τ is

$$P(F|\omega_\tau) = \frac{1}{1 + e^{-\Sigma}}. \quad (19)$$

Equation (19) demonstrates that the direction of time can be inferred more accurately by a larger entropy production. Using Eq. (12), we can obtain the upper bound of the likelihood

$$P(F|\omega_\tau) \leq \left(R^{-\mathcal{A}(\tau)(R-1)/(R+1)} N^{[-R^2 - 2R \ln(R)+1]/(R^2-1)} + 1 \right)^{-1} \quad (20)$$

for $\Sigma(\tau) > [1 + (\ln R)/(R+1)] \ln N$.

IV. CONCLUSION

In this study we derived the upper bounds for entropy production based on the dynamical activity and the maximum transition-rate ratio. We established two upper bounds, one for steady-state conditions and another for arbitrary time-dependent conditions. Furthermore, we performed numerical simulations to confirm the validity of these limits. We also identified several potential applications of the upper bounds. We expect that these findings will improve our understanding of nonequilibrium dynamics given that entropy production and dynamical activity are fundamental to thermodynamics. Finally, we discussed the application of our upper bound to real experimental data. To accurately observe the upper bound of the entropy production derived from experimental data, we must address several challenges. In real-world scenarios, observations commonly capture only a portion of a Markov chain. Consequently, we cannot calculate R , which makes it impossible to implement the proposed method directly. Resolving this issue is a topic for future studies.

ACKNOWLEDGMENT

This work was supported by JSPS KAKENHI Grant No. JP22H03659.

APPENDIX A: DERIVATION OF THE STEADY-STATE CASE

We provide a derivation of Eq. (8), which holds true under steady-state conditions. The entropy production rate σ [Eq. (4)] admits the relation

$$\begin{aligned} \sigma &= \sum_{n < m} (P_m^{\text{SS}} R_{nm} - P_n^{\text{SS}} R_{mn}) \ln \frac{P_m^{\text{SS}} R_{nm}}{P_n^{\text{SS}} R_{mn}} \\ &= \sum_{n < m} (P_m^{\text{SS}} R_{nm} - P_n^{\text{SS}} R_{mn}) \ln \frac{R_{nm}}{R_{mn}} \\ &\leq \left(\max_{m \neq n} \ln \frac{R_{nm}}{R_{mn}} \right) \sum_{n < m} |P_m^{\text{SS}} R_{nm} - P_n^{\text{SS}} R_{mn}| \\ &= \ln R \sum_{n < m} |P_m^{\text{SS}} R_{nm} - P_n^{\text{SS}} R_{mn}|, \end{aligned} \quad (A1)$$

where R is defined in Eq. (6). Using the inequality derived in Ref. [39], we obtain

$$\frac{\sigma}{f\left(\frac{\sigma}{2\alpha}\right)} \geq 2 \sum_{n < m} |P_m^{\text{ss}} R_{nm} - P_n^{\text{ss}} R_{mn}|, \quad (\text{A2})$$

where $f(x)$ is the inverse function of $x \tanh x$ as defined in the main text. Substituting Eq. (A2) into Eq. (A1), we obtain

$$\frac{\ln R}{2} \geq f\left(\frac{\sigma}{2\alpha}\right). \quad (\text{A3})$$

Because $x \tanh x$ is a monotonically increasing function, we obtain Eq. (8).

APPENDIX B: DERIVATION OF THE TIME-DEPENDENT DRIVEN CASE

Here we provide a derivation of Eq. (12). The following derivation assumes that

$$\Sigma(\tau) > \left(1 + \frac{\ln R}{R+1}\right) \ln N. \quad (\text{B1})$$

As will be shown, the assumption of Eq. (B1) is automatically satisfied by the final inequality [Eq. (B13)]. From the definition of $\Sigma(\tau)$, the following relation holds:

$$\begin{aligned} \Sigma(\tau) &= \int_0^\tau dt \sum_{n < m} [P_m(t)R_{nm}(t) - P_n(t)R_{mn}(t)] \\ &\quad \times \ln \frac{P_m(t)R_{nm}(t)}{P_n(t)R_{mn}(t)} \\ &= \int_0^\tau dt \sum_{n < m} [P_m(t)R_{nm}(t) - P_n(t)R_{mn}(t)] \ln \frac{R_{nm}(t)}{R_{mn}(t)} \\ &\quad + S(\tau) - S(0) \\ &\leq (\ln R) \int_0^\tau dt \sum_{n < m} |P_m(t)R_{nm}(t) - P_n(t)R_{mn}(t)| \\ &\quad + \ln N. \end{aligned} \quad (\text{B2})$$

Here $S(t)$ is the Shannon entropy at time t , $S(t) \equiv -\sum_n P_n(t) \ln P_n(t)$. The $S(\tau) - S(0)$ in the second line of Eq. (B2) can be derived from

$$\begin{aligned} S(\tau) - S(0) &= \int_0^\tau dt \frac{d}{dt} S(t) \\ &= \int_0^\tau dt \sum_{n < m} [P_m(t)R_{nm}(t) - P_n(t)R_{mn}(t)] \ln \frac{P_m(t)}{P_n(t)}. \end{aligned} \quad (\text{B3})$$

In the last inequality in Eq. (B2), we used the relation $0 \leq S \leq \ln N$. From Eq. (27) in Ref. [39], the following relation holds:

$$\frac{\Sigma(\tau)}{f\left(\frac{\Sigma(\tau)}{2\mathcal{A}(\tau)}\right)} \geq 2 \int_0^\tau dt \sum_{n < m} |P_m(t)R_{nm}(t) - P_n(t)R_{mn}(t)|. \quad (\text{B4})$$

Substituting Eq. (B4) into Eq. (B2), we obtain

$$\Sigma(\tau) - \ln N \leq \frac{\ln R}{2f\left(\frac{\Sigma(\tau)}{2\mathcal{A}(\tau)}\right)} \Sigma(\tau). \quad (\text{B5})$$

From Eq. (B1), the left-hand side of Eq. (B5) appears to be positive. Thus, we have

$$f\left(\frac{\Sigma(\tau)}{2\mathcal{A}(\tau)}\right) \leq \frac{\ln R}{2[\Sigma(\tau) - \ln N]} \Sigma(\tau) = \frac{\ln R}{2} [Y(\tau) + 1] \quad (\text{B6})$$

for $\Sigma(\tau) - \ln N > 0$, where

$$Y(\tau) \equiv \frac{\Sigma(\tau)}{\Sigma(\tau) - \ln N} - 1 = \frac{\ln N}{\Sigma(\tau) - \ln N} > 0. \quad (\text{B7})$$

By simply considering $f^{-1}(x)$ in Eq. (B6), we obtain

$$\frac{\Sigma(\tau)}{2\mathcal{A}(\tau)} \leq \frac{\ln R}{2} [Y(\tau) + 1] \frac{R - R^{-Y(\tau)}}{R + R^{-Y(\tau)}}. \quad (\text{B8})$$

Since $R^{-Y(\tau)} = \exp[-Y(\tau) \ln R] \geq 1 - Y(\tau) \ln R$, Eq. (B8) can be bounded as

$$\begin{aligned} \frac{\Sigma(\tau)}{2\mathcal{A}(\tau)} &\leq \frac{\ln R}{2} [Y(\tau) + 1] \frac{R - R^{-Y(\tau)}}{R + R^{-Y(\tau)}} \\ &\leq \frac{\ln R}{2} [Y(\tau) + 1] \frac{R - 1 + Y(\tau) \ln R}{R + 1 - Y(\tau) \ln R}, \end{aligned} \quad (\text{B9})$$

where we use $R + 1 - Y(\tau) \ln R > 0$ based on the assumption of Eq. (B1) and $R \geq 1$. Substituting $\Sigma(\tau) = (\ln N)[Y(\tau) + 1]/Y(\tau)$ into Eq. (B9), we obtain

$$\begin{aligned} [R + 1 - Y(\tau) \ln R] \ln N \\ \leq \mathcal{A}(\tau) Y(\tau) (\ln R) [R - 1 + Y(\tau) \ln R]. \end{aligned} \quad (\text{B10})$$

Substituting $X(\tau) = 1/Y(\tau)$ into Eq. (B10), we obtain the following quadratic equation with respect to $X(\tau)$:

$$\begin{aligned} (R + 1)(\ln N)X(\tau)^2 - [\mathcal{A}(\tau)(R - 1) + \ln N](\ln R)X(\tau) \\ - \mathcal{A}(\tau)(\ln R)^2 \equiv DX(\tau)^2 - EX(\tau) - F \leq 0. \end{aligned} \quad (\text{B11})$$

Here $D \equiv (R + 1) \ln N$, $E \equiv [\mathcal{A}(\tau)(R - 1) + \ln N] \ln R$, and $F \equiv \mathcal{A}(\tau)(\ln R)^2$, and these coefficients are all non-negative. By solving this equation with respect to $X(\tau)$, we obtain

$$X(\tau) \leq \frac{E + \sqrt{E^2 + 4DF}}{2D} \leq \frac{E}{D} + \frac{F}{E}, \quad (\text{B12})$$

where we use $\sqrt{1+x} \leq 1 + x/2$ for $x \geq 0$ in the final inequality. Substituting $X(\tau) = \Sigma(\tau)/\ln N - 1$, D , E , and F into this relation, we obtain Eq. (12) as follows:

$$\begin{aligned} \Sigma(\tau) &\leq \mathcal{A}(\tau)(\ln R) \left(\frac{R-1}{R+1}\right) \\ &\quad + \left(1 + \frac{\ln R}{R+1} + \frac{\mathcal{A}(\tau)(\ln R)}{\mathcal{A}(\tau)(R-1) + \ln N}\right) \ln N \\ &\leq \mathcal{A}(\tau)(\ln R) \left(\frac{R-1}{R+1}\right) + \left(1 + \frac{\ln R}{R+1} + \frac{\ln R}{R-1}\right) \ln N. \end{aligned} \quad (\text{B13})$$

This inequality satisfies the assumptions of Eq. (B1).

- [1] A. C. Barato and U. Seifert, Thermodynamic uncertainty relation for biomolecular processes, *Phys. Rev. Lett.* **114**, 158101 (2015).
- [2] T. R. Gingrich, J. M. Horowitz, N. Perunov, and J. L. England, Dissipation bounds all steady-state current fluctuations, *Phys. Rev. Lett.* **116**, 120601 (2016).
- [3] J. P. Garrahan, Simple bounds on fluctuations and uncertainty relations for first-passage times of counting observables, *Phys. Rev. E* **95**, 032134 (2017).
- [4] A. Dechant and S.-i. Sasa, Current fluctuations and transport efficiency for general Langevin systems, *J. Stat. Mech.* (2018) 063209.
- [5] I. Di Terlizzi and M. Baiesi, Kinetic uncertainty relation, *J. Phys. A: Math. Theor.* **52**, 02LT03 (2019).
- [6] Y. Hasegawa and T. Van Vu, Uncertainty relations in stochastic processes: An information inequality approach, *Phys. Rev. E* **99**, 062126 (2019).
- [7] Y. Hasegawa and T. Van Vu, Fluctuation theorem uncertainty relation, *Phys. Rev. Lett.* **123**, 110602 (2019).
- [8] A. Dechant and S.-i. Sasa, Fluctuation–response inequality out of equilibrium, *Proc. Natl. Acad. Sci. USA* **117**, 6430 (2020).
- [9] V. T. Vo, T. Van Vu, and Y. Hasegawa, Unified approach to classical speed limit and thermodynamic uncertainty relation, *Phys. Rev. E* **102**, 062132 (2020).
- [10] T. Koyuk and U. Seifert, Thermodynamic uncertainty relation for time-dependent driving, *Phys. Rev. Lett.* **125**, 260604 (2020).
- [11] P. Pietzonka, Classical pendulum clocks break the thermodynamic uncertainty relation, *Phys. Rev. Lett.* **128**, 130606 (2022).
- [12] K. Brandner, T. Hanazato, and K. Saito, Thermodynamic bounds on precision in ballistic multiterminal transport, *Phys. Rev. Lett.* **120**, 090601 (2018).
- [13] F. Carollo, R. L. Jack, and J. P. Garrahan, Unraveling the large deviation statistics of Markovian open quantum systems, *Phys. Rev. Lett.* **122**, 130605 (2019).
- [14] G. Guarneri, G. T. Landi, S. R. Clark, and J. Goold, Thermodynamics of precision in quantum nonequilibrium steady states, *Phys. Rev. Res.* **1**, 033021 (2019).
- [15] S. Saryal, H. M. Friedman, D. Segal, and B. K. Agarwalla, Thermodynamic uncertainty relation in thermal transport, *Phys. Rev. E* **100**, 042101 (2019).
- [16] Y. Hasegawa, Quantum thermodynamic uncertainty relation for continuous measurement, *Phys. Rev. Lett.* **125**, 050601 (2020).
- [17] M. F. Sacchi, Thermodynamic uncertainty relations for bosonic Otto engines, *Phys. Rev. E* **103**, 012111 (2021).
- [18] A. A. S. Kalaei, A. Wacker, and P. P. Potts, Violating the thermodynamic uncertainty relation in the three-level maser, *Phys. Rev. E* **104**, L012103 (2021).
- [19] T. Koyuk and U. Seifert, Thermodynamic uncertainty relation in interacting many-body systems, *Phys. Rev. Lett.* **129**, 210603 (2022).
- [20] Y. Hasegawa, Unifying speed limit, thermodynamic uncertainty relation and Heisenberg principle via bulk-boundary correspondence, *Nat. Commun.* **14**, 2828 (2023).
- [21] N. Shiraishi, K. Funo, and K. Saito, Speed limit for classical stochastic processes, *Phys. Rev. Lett.* **121**, 070601 (2018).
- [22] S. Ito, Stochastic thermodynamic interpretation of information geometry, *Phys. Rev. Lett.* **121**, 030605 (2018).
- [23] A. Dechant and Y. Sakurai, Thermodynamic interpretation of Wasserstein distance, [arXiv:1912.08405](https://arxiv.org/abs/1912.08405).
- [24] S. Ito and A. Dechant, Stochastic time evolution, information geometry, and the Cramér-Rao bound, *Phys. Rev. X* **10**, 021056 (2020).
- [25] S. B. Nicholson, L. P. Garcia-Pintos, A. del Campo, and J. R. Green, Time-information uncertainty relations in thermodynamics, *Nat. Phys.* **16**, 1211 (2020).
- [26] T. Van Vu and Y. Hasegawa, Geometrical bounds of the irreversibility in Markovian systems, *Phys. Rev. Lett.* **126**, 010601 (2021).
- [27] M. Nakazato and S. Ito, Geometrical aspects of entropy production in stochastic thermodynamics based on Wasserstein distance, *Phys. Rev. Res.* **3**, 043093 (2021).
- [28] L. Mandelstam and I. Tamm, The uncertainty relation between energy and time in non-relativistic quantum mechanics, *J. Phys. USSR* **9**, 249 (1945).
- [29] N. Margolus and L. B. Levitin, The maximum speed of dynamical evolution, *Physica D* **120**, 188 (1998).
- [30] S. Deffner and S. Campbell, Quantum speed limits: From Heisenberg’s uncertainty principle to optimal quantum control, *J. Phys. A: Math. Theor.* **50**, 453001 (2017).
- [31] U. Seifert, From stochastic thermodynamics to thermodynamic inference, *Annu. Rev. Condens. Matter Phys.* **10**, 171 (2019).
- [32] J. Li, J. M. Horowitz, T. R. Gingrich, and N. Fakhri, Quantifying dissipation using fluctuating currents, *Nat. Commun.* **10**, 1666 (2019).
- [33] S. K. Manikandan, D. Gupta, and S. Krishnamurthy, Inferring entropy production from short experiments, *Phys. Rev. Lett.* **124**, 120603 (2020).
- [34] É. Roldán, J. Barral, P. Martin, J. M. R. Parrondo, and F. Jülicher, Quantifying entropy production in active fluctuations of the hair-cell bundle from time irreversibility and uncertainty relations, *New J. Phys.* **23**, 083013 (2021).
- [35] S. Limkumnerd, Upper bound for the average entropy production based on stochastic entropy extrema, *Phys. Rev. E* **95**, 032125 (2017).
- [36] I. Neri, E. Roldán, and F. Jülicher, Statistics of infima and stopping times of entropy production and applications to active molecular processes, *Phys. Rev. X* **7**, 011019 (2017).
- [37] D. S. P. Salazar, Upper bound for quantum entropy production from entropy flux, *Phys. Rev. E* **105**, L042101 (2022).
- [38] I. Di Terlizzi, M. Gironella, D. Herráez-Aguilar, T. Betz, F. Monroy, M. Baiesi, and F. Ritort, Variance sum rule for entropy production, [arXiv:2302.08565](https://arxiv.org/abs/2302.08565).
- [39] V. T. Vo, T. V. Vu, and Y. Hasegawa, Unified thermodynamic-kinetic uncertainty relation, *J. Phys. A: Math. Theor.* **55**, 405004 (2022).
- [40] A. C. Barato and U. Seifert, Cost and precision of Brownian clocks, *Phys. Rev. X* **6**, 041053 (2016).
- [41] T. Nishiyama, Thermodynamic-kinetic uncertainty relation: Properties and an information-theoretic interpretation, [arXiv:2207.08496](https://arxiv.org/abs/2207.08496).
- [42] R. Spinney and I. Ford, in *Nonequilibrium Statistical Physics of Small Systems*, edited by R. Klages, W. Just, and C. Jarzynski (Wiley, New York, 2013), Chap. 1, pp. 3–56.
- [43] C. Jarzynski, Equalities and inequalities: Irreversibility and the second law of thermodynamics at the nanoscale, *Annu. Rev. Condens. Matter Phys.* **2**, 329 (2011).
- [44] A. Seif, M. Hafezi, and C. Jarzynski, Machine learning the thermodynamic arrow of time, *Nat. Phys.* **17**, 105 (2021).